Article published online: 2021-07-27

Spinal dysraphism illustrated; Embroyology revisited

Ullas V Acharya, Hima Pendharkar[1], Dandu R Varma[3], Nupur Pruthi[2], Shriram Varadarajan[4]

Department of Radiology, Manipal Hospital, Departments of [1]Neuroimaging and Interventional Radiology, [2]Neurosurgery, National Institute of Mental Health and Neurosciences, Bengaluru, Karnataka, [3]Citi Neuro Centre, Mediciti Hospital, Hyderabad, Telangana, [4]Department of Radiology, Christian Medical College, Ludhiana, Punjab, India

Correspondence: Dr. Ullas V Acharya, Department of Radiology, Manipal Hospital, HAL Road, Bengaluru, Karnataka, India.
E-mail: ullasva77@gmail.com

Abstract

Spinal cord development occurs through three consecutive periods of gastrulation, primary nerulation and secondary neurulation. Aberration in these stages causes abnormalities of the spine and spinal cord, collectively referred as spinal dysraphism. They can be broadly classified as anomalies of gastrulation (disorders of notochord formation and of integration); anomalies of primary neurulation (premature dysjunction and nondysjunction); combined anomalies of gastrulation and primary neurulation and anomalies of secondary neurulation. Correlation with clinical and embryological data and common imaging findings provides an organized approach in their diagnosis.

Key words: Embryology; illustrated; magnetic resonance imaging; spinal dysraphism

Introduction

Spinal dysraphism refers to the congenital abnormalities of the spine and spinal cord. Clinico-radiological classification of spinal dysraphism has been well established and widely followed. The objective of this article is to illustrate the common magnetic resonance imaging (MRI) findings of various spinal dysraphisms based on embryological events.[1-3]

Spinal Cord Development

Spinal cord development can be summarized in three basic embryologic stages – gastrulation (2–3 weeks), primary neurulation (3-4 weeks) and secondary neurulation (5–6 weeks).[4,5] The rostral spinal cord (to about the level of S2) is formed by primary neurulation and the caudal spinal cord (distal to S2 level) by secondary neurulation, also referred to as canalization and retrogressive differentiation.[6]

Gastrulation

Gastrulation is the process of conversion of bilaminar disc into a trilaminar disc initiated by primitive streak [Figure 1]. Primitive node, a depression at the cranial end of streak, contains cells that are important for organizing the embryonic axes. Epiblast cells migrate toward and through the streak and node, detach and form two new layers ventral to the remaining epiblast. The first cells through the streak displace the original hypoblast to form endoderm, whereas cells migrating slightly later create a new middle layer, the mesoderm. Nonmigrating cells of epiblast constitute the ectoderm. Some cells migrate cranially in the midline to form the prechordal plate and notochord, which initiate

Access this article online	
Quick Response Code:	Website: www.ijri.org
	DOI: 10.4103/ijri.IJRI_451_16

Cite this article as: Acharya UV, Pendharkar H, Varma DR, Pruthi N, Varadarajan S. Spinal dysraphism illustrated; Embroyology revisited. Indian J Radiol Imaging 2017;27:417-26.

the process of neurulation by inducing the formation of the neural plate from overlying ectoderm cells. Thus, neural plate is derived from ectoderm and forms in the central part of this upper layer. Remainder of the ectoderm surrounding the neural plate forms the epidermis.[7]

Primary Neurulation

Lateral borders of neural plate elevate into neural folds which later fuse in the midline to form the neural tube [Figure 2]. The open regions of the neural tube called the anterior (cranial) and posterior (caudal) neuropores close by the zippering process. This neurulation process is called primary neurulation which is responsible for establishing brain and spinal cord regions down to the sacral levels (probably up to S2). On neural tube closure, overlying non-neural epidermal cells form the ectodermal layer of the skin. Normal neural tube closure occurs by day 25 to 27.[7] Meanwhile, the neural tube separates from the overlying ectoderm, a process called dysjunction.

The neuroepithelial cells (neuroblasts) around the inner neural tube form the mantle layer, which produces the spinal cord gray matter. The outermost layer forms the marginal layer, which subsequently myelinates to produce the spinal cord white matter. The central neuroepithelial cells differentiate into ependymal cells along the central canal. Neural crest cells along each side of the neural tube form the dorsal root ganglia, autonomic ganglia, Schwann cells, leptomeninges and adrenal medulla.[6]

Secondary Neurulation

The cord caudal to S2 level is formed by this process. Totipotent mesodermal cells called caudal cell mass or tail bud coalesce to form neural tube which then epithelialize, reorganize around a lumen and finally become continuous with the cranial part of the tube initially formed by primary neurulation.[7,8] Part of the caudal cell mass undergoes both regression and differentiation (a process called retrogressive differentiation) to form filum terminale, terminal ventricle, tip of conus medullaris, and most of the sacrum, coccyx and coccygeal medullary vestige [Figure 3].[9] By the third gestational month, spinal cord extends the entire length of the developing spinal column. Rapid elongation of the vertebral column and dura relative to the cord produces the apparent ascent of the cord during the remainder of the gestation and the conus is at the adult level soon after birth.

Spinal dysraphism can be classified based on embryological events, as shown in the Table 1, which is formatted based on studies by Tortori and Caffey.[4,6]

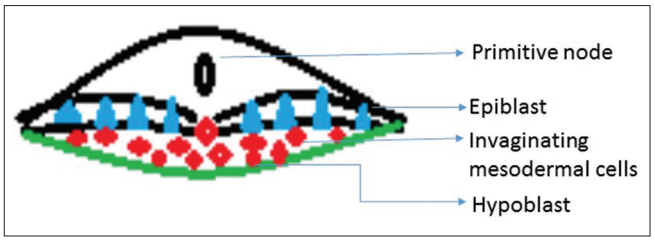

Figure 1: Gastrulation – Process of formation of trilaminar disc

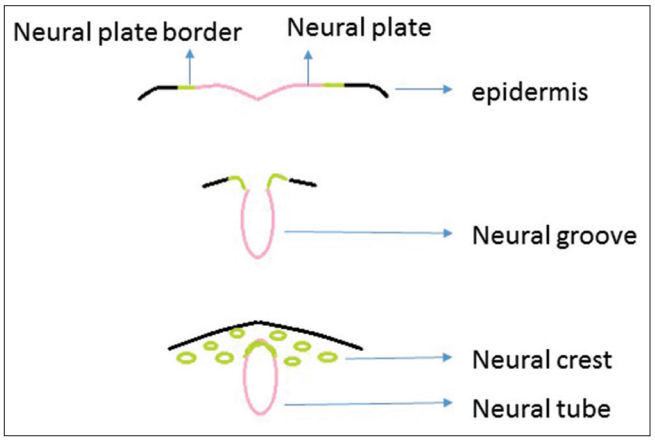

Figure 2: Primary neurulation – Neural plate folds on itself to form a neural tube which closes in a zipper-like manner and separates from the overlying surface ectoderm which forms the epidermis

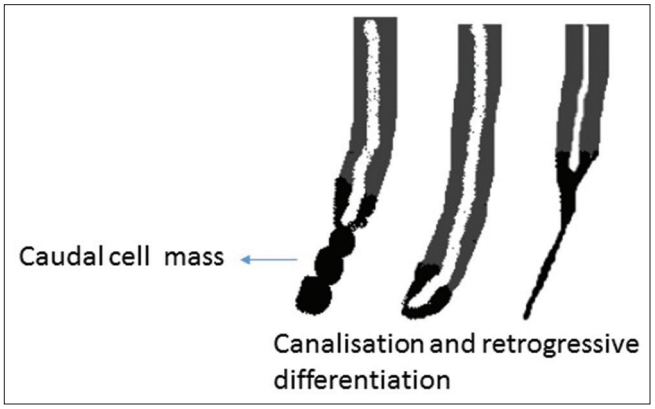

Figure 3: Secondary neurulation – Caudal cell mass coalesces, becomes continuous with the cranial part of the tube initially formed by primary neurulation, and undergoes both regression and differentiation, a process called retrogressive differentiation

Clinical manifestations include abnormal cutaneous manifestations, neurological deficits including gait disturbance and bowel and bladder incontinence. Cutaneous markers are reported to be present in 50–80% of the patients. These lesions are usually already evident at birth, which can point to the underlying pathology. Cutaneous markers are classified based on the index of suspicion of underlying spinal dysraphism as follows [Table 2; Figures 4 and 5].[10]

Clinico-radiologically, spinal dysraphism is classified into two categories. The first category is spinal dysraphism with back mass that is not covered by skin, i.e. open dysraphism.

Table 1: Embryological classification of spinal dysraphism with salient features

A	**Anomalies of Gastrulation**	
1	**Disorders of Notochord Formation**	
a	Caudal Regression Syndrome	Lumbosacral vertebral body dysgenesis/hypogenesis Truncated blunt spinal cord terminating above the expected level
b	Segmental Spinal Dysgenesis	Congenital thoracic or lumbar kyphosis Bulky, thickened and low lying cord below the dysgenetic segment
2	**Disorders Of Notochord Integration**	
a	Neurenteric cysts	Separation failure resulting in an abnormal connection between primitive endoderm and ectoderm resulting in trapping of a small piece of primitive gut within the developing spinal canal which may become isolated forming a cyst or may maintain connections with gut or skin (or both); producing the spectrum of dorsal-enteric spinal anomalies
b	Dorsal enteric fistula	
c	Split cord malformations [diastematomyelia]	Splitting of the spinal cord into two hemicords In type 1, the two hemicords are located within individual dural tubes separated by an osseous or cartilaginous septum and in type 2, there is a single dural tube containing two hemi-cords
B	**Anomalies of Primary Neurulation**	
1	**Premature Dysjunction**	
a	Lipomyelomeningocele	Closed dysraphism with skin-covered lumbosacral masses The placode–lipoma interface lies outside of the spinal canal due to expansion of the sub-arachnoid space
b	Lipomyelocele	Closed dysraphism with skin-covered lumbosacral masses The placode–lipoma interface lies within the spinal canal
c	Intradural lipoma	Closed dysraphism Lipoma located along the dorsal midline that is contained within the dural sac Lumbosacral most common location
2	**Nondysjunction**	
a	Dorsal dermal sinus	Tract connecting skin dimple to the dural sac, conus or central spinal cord canal True congenital dorsal DST usually has an atypical dimple at the ostium that is larger (>5 mm), often asymmetric, and remote (>2.5 cm) from the anus
b	Myelomeningocele	Open dysraphism Neural placode protrudes above the skin surface Almost always associated with Chiari 2 malformation
c	Myelocele	Open dysraphism Neural placode is in flush with the skin surface with a myelocele
C	**Combined Anomalies of Gastrulation and Primary Neurulation**	
1	Hemimyelocele	Extremely rare
2	Hemimyelomeningocele	Diastematomyelia associated with myelomeningocele or myelocele of one of the hemicords
D	**Anomalies of Secondary Neurulation and Retrogressive Differentiation**	
1	Abnormally long spinal cord	Persistent cord termination below L2-L3 after the first month of life in a full-gestation infant
2	Persisting terminal ventricle	Location immediately above filum terminale Lack of contrast enhancement Usually does not have pathological significance during the first 5 years of life
3	Tight filum terminale	Low-lying cord with thickened filum.
4	Intrasacral – anterior sacral meningocele	Intrasacral meningocele – sac lined by arachnoid which lies within an enlarged sacral spinal canal attached to the caudal termination of the dural sac Anterior sacral meningocele – Large anterior meningocele outpouching that traverses an enlarged sacral foramen and produces a presacral cystic mass. Inherited predisposition within the Currarino triad
5	Terminal myelocystocele	Herniation of large terminal syrinx (syringocele) into a posterior meningocele through a posterior spinal defect which do not usually communicate with each other

The second is spinal dysraphism with skin-covered back mass, i.e. closed dysraphism, which can be further subcategorized on the basis of the presence or absence of a subcutaneous mass.[11,12]

Anomalies of Gastrulation

Failure of notochord formation causes complex dysraphic states such as caudal regression syndrome and segmental spinal dysgenesis. Incorrect notochordal induction leads to the incomplete splitting of the neural plate from the notochord, producing the split notochord syndromes (neurenteric cyst and diastematomyelia).

Anomalies of notochord formation

Caudal regression syndrome

Caudal regression syndrome (CRS) is a complex dysraphic state with aberrations in gastrulation, secondary as well as

Table 2: Classification of cutaneous markers based on index of suspicion of underlying spinal dysraphism

High Index of Suspicion	Low Index of Suspicion
Hypertrichosis	Telangiectasia
Dimples (large, >2.5 cm from the anal verge, atypical)	Capillary malformation (port-wine stain)
Acrochordons/pseudotails/true tails	Hyperpigmentation
Lipomas	Melanocytic nevi
Hemangiomas	Teratomas
Aplasia cutis or scar	
Dermoid cyst or sinus	

primary neurulation.[13,14] Most cases are sporadic, although a dominantly inherited defect in the *HLXB9* gene has been described.[14] Mothers of 15–20% of these infants are diabetic, and the offspring of 1% diabetic mothers are afflicted. Associations with other caudal spinal segment anomalies such as vertebral segmentation and formation anomalies and split cord malformations are noted.

Two types are described. Type 1 features a foreshortened terminal vertebral column, high-lying wedge-shaped conus termination and more severe associated visceral and orthopedic anomalies. Type 2 is less severe and has a low-lying tethered spinal cord with milder associated malformations [Figure 6] In general, the higher the cord termination, the more severe is the sacral anomalies. The most severe CRS presentations are lumbosacral agenesis in which the spine terminates at the lower thoracic level and there is severe sacral dysgenesis with fused lower extremities in a "mermaid" configuration (sirenomyelia).[6]

Segmental spinal dysgenesis

Segmental spinal dysgenesis (SSD) is a very rare dysraphic anomaly characterized by segmental thoracolumbar or lumbar vertebral and spinal cord dysgenesis or agenesis. Congenital thoracic or lumbar kyphosis is characteristic, with a palpable dorsal bone spur located at the gibbous apex.[15] The upper spinal cord is normal, however, the cord segment below the dysgenetic segment is bulky, thickened and low-lying. The spinal canal proximal and distal to the dysgenetic level is of normal caliber [Figure 7].

Anomalies of notochord induction

Neurenteric cyst and dorsal-enteric spinal anomalies

Neurenteric cyst (NEC) is a complex dysraphic state and consists of an intraspinal cyst lined by enteric mucosa. It is most common in thoracic spine followed by cervical spine. They arise from an abnormal connection between primitive endoderm and ectoderm that persists beyond the third embryonic week. Normally, the notochord separates ventral endoderm (foregut) and dorsal ectoderm (skin, spinal cord) during embryogenesis, in an NEC, a separation failure "splits" the notochord and hinders the development of mesoderm, which traps a small piece of primitive gut within the developing spinal canal. This gut remnant may become isolated forming a cyst or it may maintain connections with gut or skin (or both); this produces the spectrum of fistulas

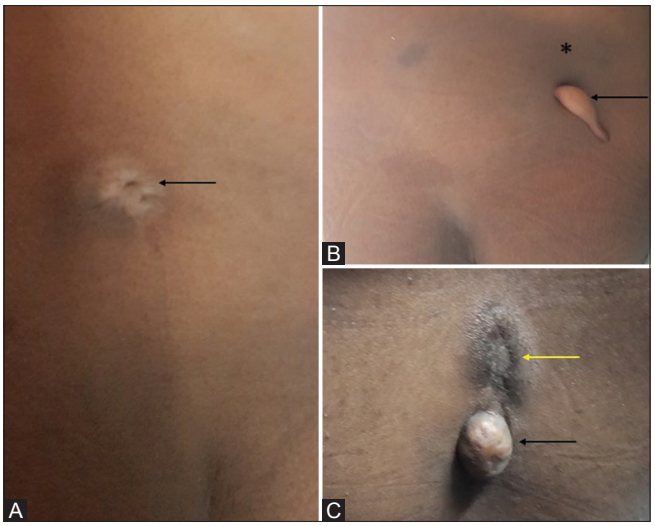

Figure 4 (A-C): Cutaneous manifestations – (A) Atrophic patch with dermal sinus (arrow); (B) Pseudotail (arrow) with hyperpigmentation (*). (C) Lipoma (black arrow) with dermal sinus (yellow arrow)

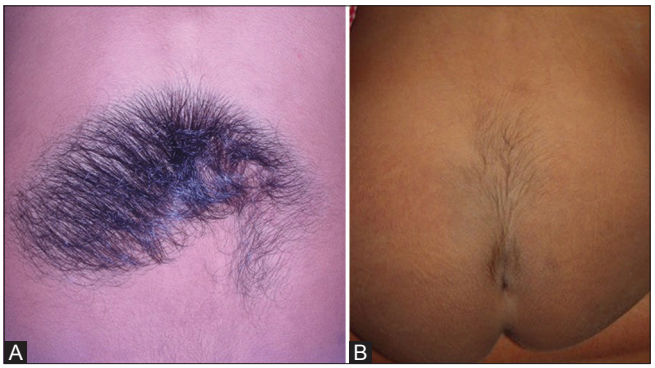

Figure 5 (A and B): Hypertrichosis – (A) Silky down type – short and fine vellus hairs. (B) Faun tail type – long coarse terminal hairs

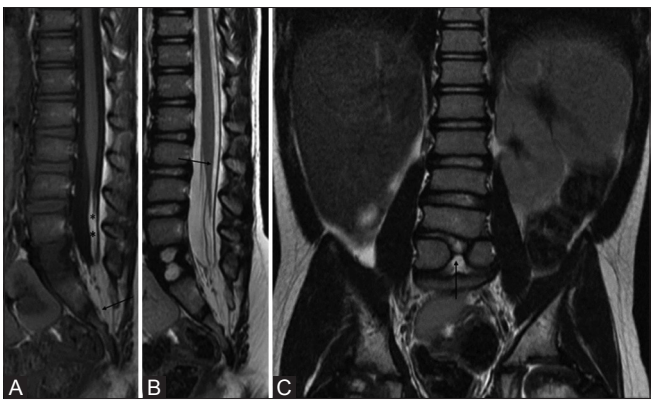

Figure 6 (A-C): Partial sacral agenesis – Sagittal T1 (A) and Sagittal T2 (B) weighted images of lumbosacral spine showing partial agenesis of sacrum (arrow in A), low lying cord (arrow in B) and lipomatous thickening of filum terminale (*in A). Coronal T2 (C) image demonstrates L5 butterfly vertebra (arrow)

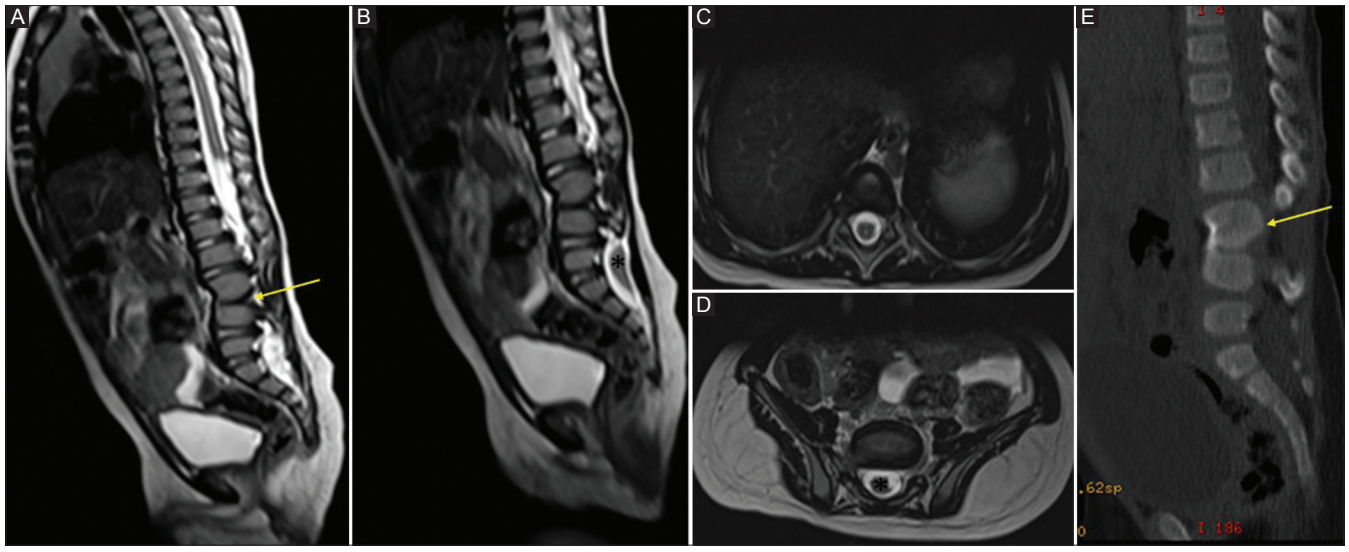

Figure 7 (A-E): Segmental spinal dysgenesis – Sagittal T2-weighted (A and B), axial T2-weighted (C and D), and sagittal CT reconstruction (E) of lumbosacral spine shows focal lumbar kyphotic deformity (arrow in A and E) with indiscernible spinal cord at the same level, normal spinal canal dimension of cranial segment (C) and bulky low lying caudal cord segment (*in B and D)

and sinuses that constitute the spectrum of dorsal-enteric spinal anomalies.

Most severe malformations remain in communication through the primitive vertebral osseous canal of Kovalevsky, however, even mild cases usually show some vertebral segmentation anomalies on close inspection [Figure 8].

Diastematomyelia

Diastematomyelia is the separation of the spinal cord into two hemicords. Diastematomyelia can present clinically with scoliosis and tethered-cord syndrome. A hairy tuft on the patient's back can be a distinctive finding on physical examination [Figure 5]. There are two types of diastematomyelia. In type 1, the two hemicords are located within individual dural tubes separated by an osseous or cartilaginous septum [Figure 9]. In type 2, there is a single dural tube containing two hemi-cords, sometimes with an intervening fibrous septum [Figure 10].[16]

Abnormalities of Primary Neurulation

Premature dysjunction

If dysjunction occurs prematurely, perineural mesenchyme is interposed between neural tube and ectoderm, which may differentiate into fat and prevent complete neural tube closure. It leads to the lipomatous malformation spectrum of lipomyelocele, lipomyelomeningocele and spinal lipomas.[6]

Lipomyelocele (LMC), b) lipomyelomeningocele (LMMC)

The main differentiating feature between a LMC and LMMC is the position of the placode–lipoma interface.[11] With an LMC, the placode–lipoma interface lies within the spinal canal. With an LMMC, the placode–lipoma interface lies outside of the spinal canal due to expansion of the sub-arachnoid space [Figures 11 and 12].[12] In both cases, syringomyelia is a commonly associated finding. LMC and LMMC account for 20–56% of occult spinal dysraphism and 20% of skin-covered lumbosacral masses. An important imaging point is that the neural placode is frequently rotated; this foreshortens the roots on one side, predisposing them to stretch injury, and lengthens the roots on the other side, rotating them into the surgeon's field of view and making them more prone to injury.

The spinal lipoma

The spinal lipoma is a simple dysraphic state and is subdivided into intradural and terminal (filar) lipomas. An intradural lipoma refers to a lipoma located along the dorsal midline that is contained within the dural sac [Figure 13]. No open spinal dysraphism is present. They are most commonly lumbosacral in location.[17] Fibrolipomatous thickening of the filum terminale is referred to as a filar lipoma [Figure 14]. Filar lipomas can be considered a normal variant if there is no clinical evidence of tethered-cord syndrome.[18,19]

Nondysjunction

Nondysjunction results from failure of dissociation of neural tube from adjacent cutaneous tissue. If dysjunction fails to occur, an ectodermal–neuroectodermal tract forms that prevents mesenchymal migration. Nondysjunction results in open neural tube defect spectrum of dorsal dermal sinus, myelomeningocele, and myeloceles.

Dorsal dermal sinus

The simplest of these is the dorsal dermal sinus connecting skin dimple to the dural sac, conus, or central spinal cord canal. The most common dermal sinus tract (DST) location

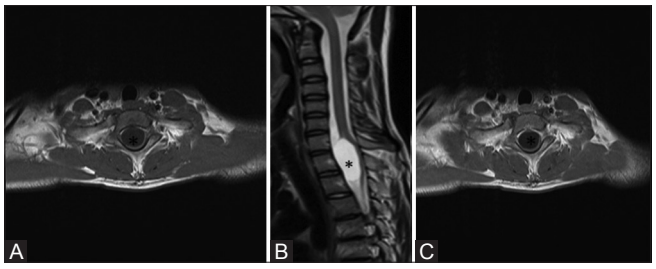

Figure 8 (A-C): Neurenteric cyst – Axial T1-weighted (A) and sagittal T2-weighted (B) MR images show a cyst (*) located in anterior subarachnoid space opposite C7-T2 vertebra. It shows no enhancement on axial T1 post contrast (C)

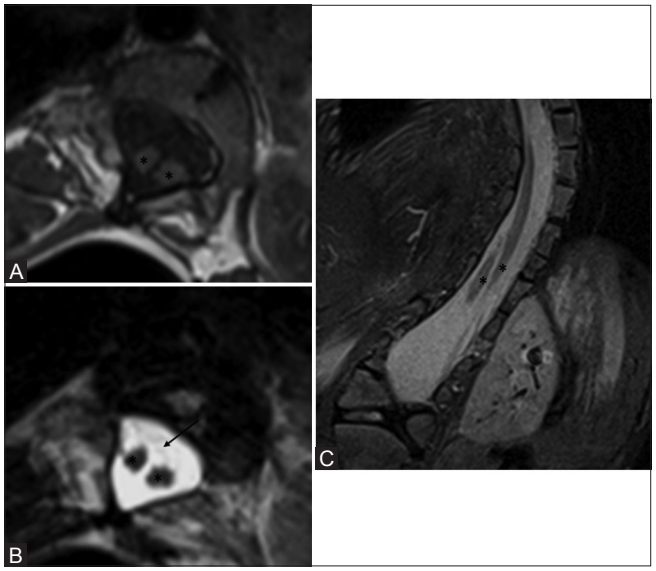

Figure 10 (A-C): Type 2 diastematomyelia – Axial T1-weighted (A), axial T2-weighted (B), coronal STIR (C) MR images show splitting of distal cord into two hemicords (*) within single dural tube (arrow in B)

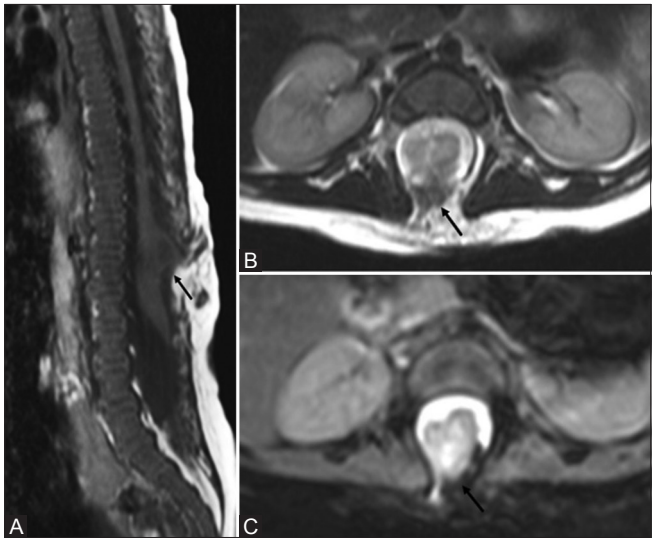

Figure 12 (A-C): Lipomyelomeningocele – Sagittal T1-weighted (A) and axial T2-weighted images (B) of lipomyelomeningocele shows placode–lipoma interface (arrow) lying outside the spinal canal due to expansion of subarachnoid space. There is suppression of lipoma at interface as seen on axial T2 STIR images (C)

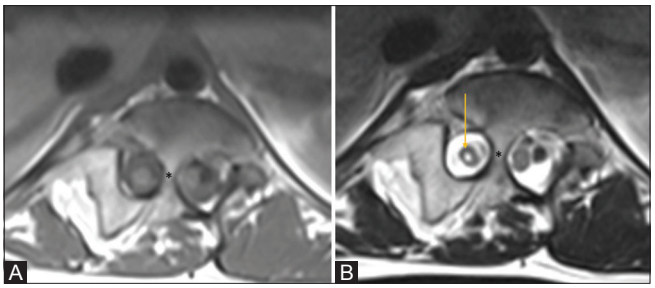

Figure 9 (A and B): Type 1 diastematomyelia – Axial T1-weighted (A) and axial T2-weighted (B) MR images show two dural tubes separated by osseous bridge (*) at L1 vertebral level. Syrinx is noted within right hemicord (yellow arrow)

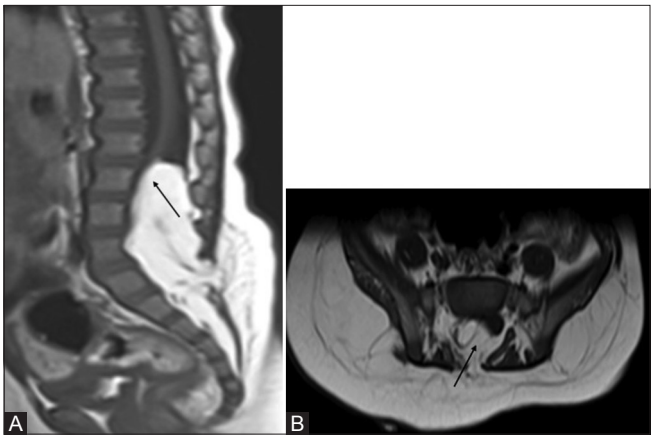

Figure 11 (A and B): Lipomyelocele – Sagittal T1 (A) and axial T2 images (B) of lipomyelocele shows placode–lipoma interface lying within spinal canal (arrow)

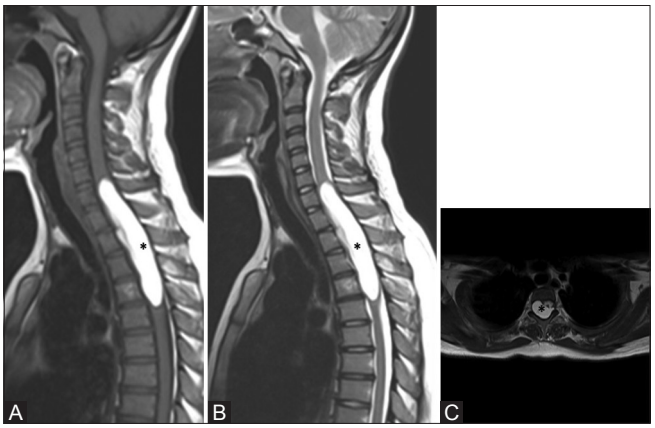

Figure 13 (A-C): Intradural lipoma – Sagittal T1-weighted (A), sagittal T2-weighted (B), and axial T2-weighted (C) MR images show large intradural lipoma (*) opposite C7 to D4 vertebral level. It is hyperintense on T1 and T2-weighted image and showed suppression on T2-weighted fat-saturated image (not shown)

is in the lumbosacral spine, followed by the occiput. In all dermal sinus cases, there is some degree of focal dysraphism, which may be as subtle as a bifid spinous process. The true congenital dorsal DST usually has an atypical dimple at the ostium that is large (>5 mm), often asymmetric, and remote (>2.5 cm) from the anus [Figure 4A]. These

features help distinguish the dermal sinus from its clinically asymptomatic mimic, simple coccygeal dimple.[20,21] The sinus tract/cord is epithelial-cell lined and may or may not be canalized. When patent, it exposes the patient to an elevated risk of meningitis. It is critical to look for this anomaly in all patients with atypical skin dimples, cutaneous back lesions or lipomas. Moreover, 30–50% of DSTs may have an associated dermoid or epidermoid cyst [Figures 15-17].

Myelomeningocele and myelocele

Myelomeningoceles and myeloceles are caused by defective closure of the primary neural tube and are clinically characterized by exposure of the neural placode through a midline skin defect on the back, and hence, classified under open dysraphic states. Myelomeningoceles account for more than 98% of open spinal dysraphisms. Myeloceles are rare. It is important to note that preoperative imaging of myelomeningocele is usually not done because of the risk of infection. Nevertheless, the main differentiating imaging feature between a myelomeningocele and myelocele is the position of the neural placode relative to the skin surface. The neural placode protrudes above the skin surface with a myelomeningocele [Figure 18] and is flush with the skin

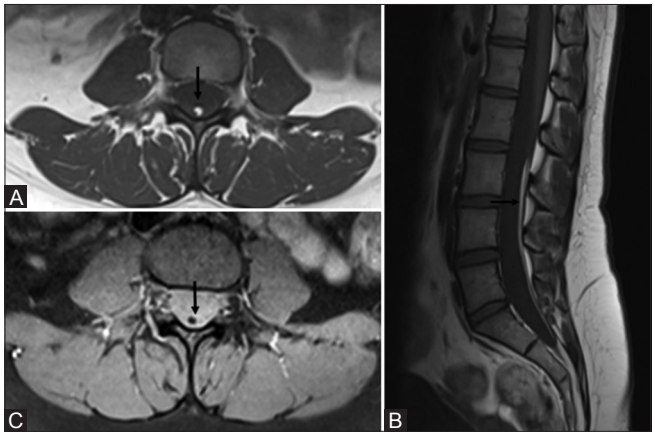

Figure 14 (A-C): Filar lipoma – Axial T1 (A) and sagittal T1 (B) weighted MR images show thickened hyperintense filum terminale which suppresses on axial fat saturated image (C) (arrow)

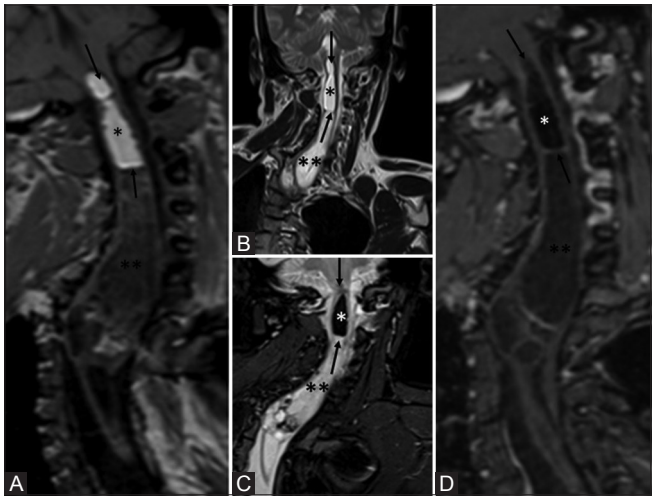

Figure 16 (A-D): Dermoid cyst – coronal T1-weighted (A), coronal T2-weighted (B), coronal STIR (C), and Coronal T1FS postcontrast (D) sequences show a long segment heterogeneous lesion causing expansion of cord. Cranial part of the lesion (limited by arrows) shows fat signals (*) whereas larger caudal part of the lesion is predominantly cystic and shows peripheral enhancement (**)

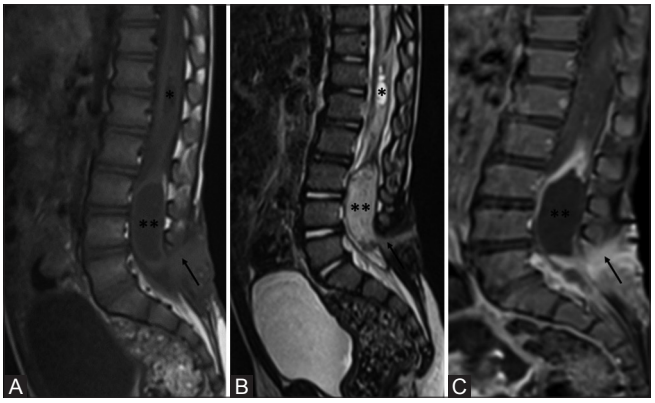

Figure 15 (A-C): Dorsal dermal sinus with epidermoid cyst – sagittal T1-weighted (A), sagittal T2 weighted (B), and sagittal T1 postcontrast FS (C) images show a T1 hypointense, T2 hyperintense sinus tract (arrow) at L5 level, which shows diffuse homogenous postcontrast enhancement. Associated peripherally enhancing T1 hypointense, T2 hyperintense epidermoid cyst (**) is noted opposite L3-5 level with focal cord syrinx (*) and T2 hyperintense signals at D12–L1

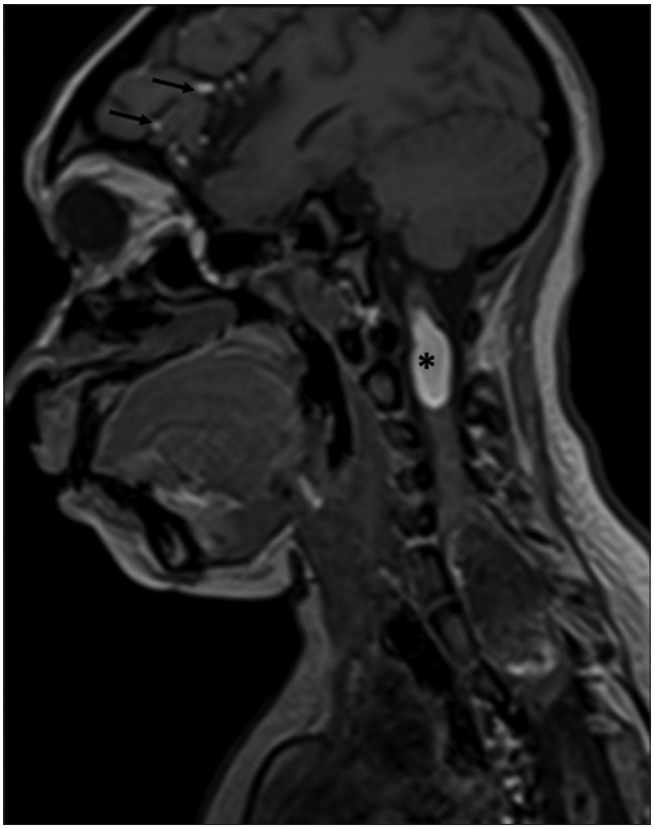

Figure 17: Ruptured dermoid cyst – sagittal T1-weighted image shows cervical T1 hyperintense lesion (*). Note multiple small T1 hyperintense punctate foci along sylvian fissure and frontal lobe sulci (arrows)

surface with a myelocele. Myelomeningocele is almost always seen in the context of a Chiari 2 malformation.[4,17,22]

Combined Anomalies of Gastrulation and Primary Neurulation

Hemimyelomeningocele and hemimyelocele

Hemimyelomeningoceles and hemimyeloceles can also occur but are extremely rare. These conditions occur when a myelomeningocele or myelocele is associated with diastematomyelia (cord splitting) and one hemicord fails to neurulate [Figure 19].

Anomalies of Secondary Neurulation/Anomalies of the Caudal Cell Mass

Failure of expected secondary neurulation leads to conditions such as abnormally long spinal cord, tethered cord syndrome, persisting terminal ventricle, terminal myelocystocele, lipoma of filum terminale and intrasacral – anterior sacral meningocele. It is also implicated in pathogenesis of caudal regression syndrome and segmental spinal dysgenesis.[6]

Low lying cord

Persistent cord termination below L2–L3 after the first month of life in a full-gestation infant is abnormally low-lying. Axial T1-weighted images are most accurate in determining the conus level [Figure 20].[23,24]

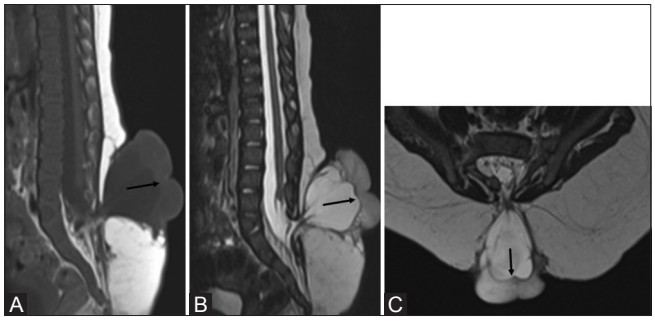

Figure 18 (A-C): Myelomeningocele – sagittal T1 (A), T2 (B), and axial T2 (C) weighted images show low lying cord with neural placode (arrow) protruding above skin surface due to expansion of underlying subarachnoid space

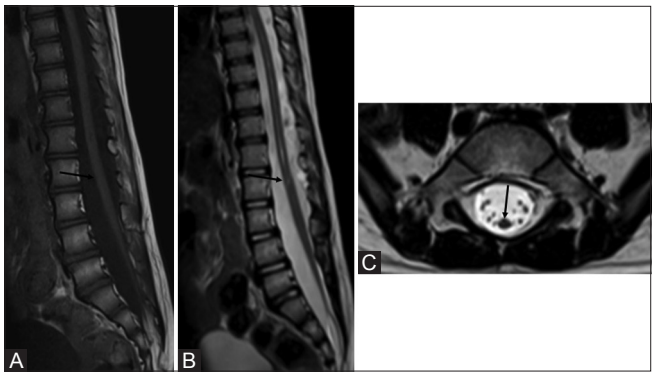

Figure 20 (A-C): Low lying tethered cord – sagittal T1 (A), sagittal T2 (B), and axial T2-weighted (C) images show low lying tethered cord (arrow in A and B) with thickened filum terminale (arrow in C) at S1 level (arrow in C)

Persistent terminal ventricle/fifth ventricle

By day 48, a transient ventriculus terminalis appears in the future conus. According to Coleman *et al.*, evidence of a fifth ventricle not accompanied by other pathologies is a frequent finding that does not have pathological significance during the first 5 years of life.[25] Key imaging features include location immediately above filum terminale and lack of contrast enhancement, which differentiates this entity from other cystic lesions of the conus medullaris.

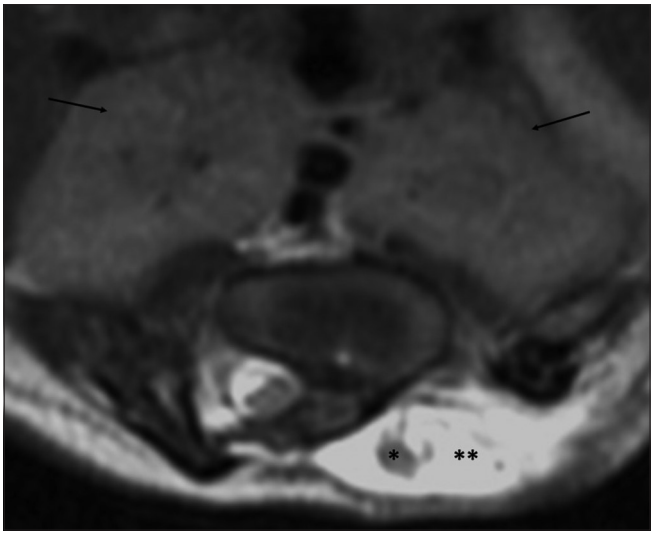

Figure 19: Hemimyelomeningocele – axial T2-weighted image shows type 1 diastometamyelia with the left hemicord (*) seen ending within a myelomeningocele sac (**). Note also malpositioned, malaligned kidneys (arrows)

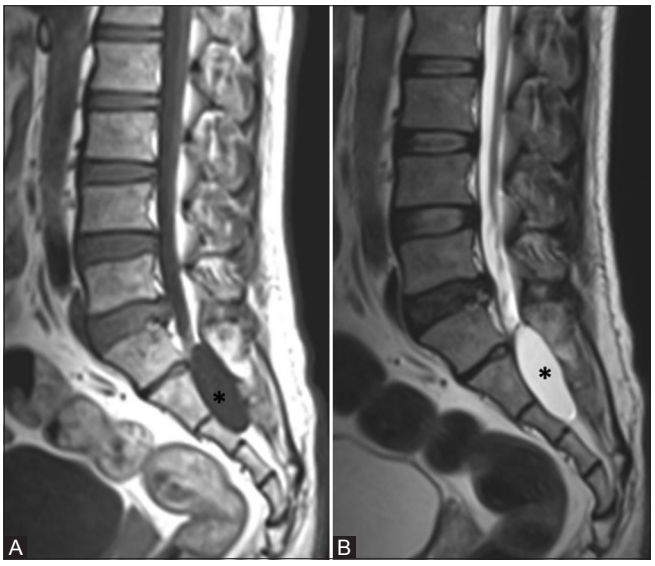

Figure 21 (A and B): Intrasacral meningocele – sagittal T1-weighted (A) and sagittal T2-weighted (B) images show CSF intensity lesion (*) in sacral canal

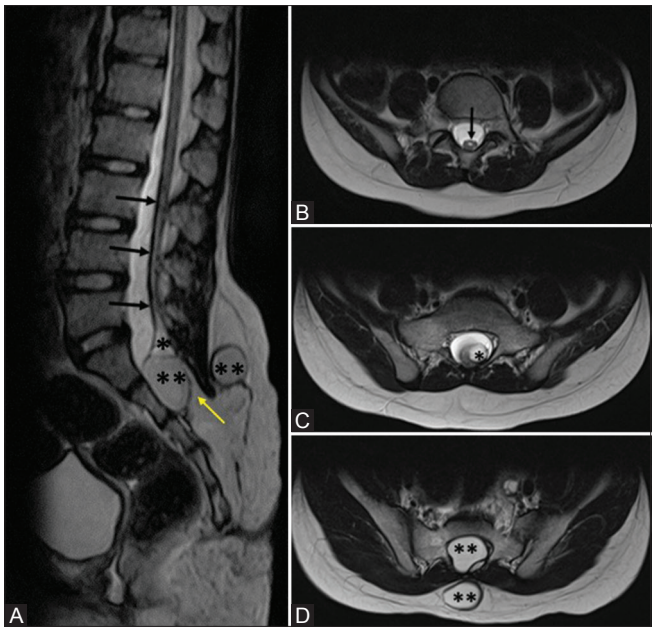

Figure 22 (A-D): Terminal myelocystocele with lipomyelocele – sagittal T2-weighted image (A) and axial T2-weighted images (B-D) show syrinx involving lower cord (arrows in A and B), focal terminal flaring of syrinx (* in A and C) surrounded by pockets of meningoceles (** in A and D). Liponeural junction is shown with yellow arrow in A

Tethered cord syndrome

Tethered cord syndrome (TCS) patients most likely present during periods of rapid somatic growth. It manifests clinically as gait spasticity, low back and leg pain that is worse in the morning, lower extremity sensory abnormalities, and/or bladder difficulties. On imaging, TCS strictly refers to patients with a low-lying cord and thickened filum [>1.5 mm] [Figure 20].

Intrasacral – anterior sacral meningocele

The term "intrasacral meningocele" is used to denote a sac lined by arachnoid which lies within an enlarged sacral spinal canal and is attached to the caudal termination of the dural sac by a pedicle that usually permits cerebrospinal fluid (CSF) flow from the tip of the subarachnoid space into the meningocele. Consistent with the possible congenital origin, intrasacral meningocele may occur in association with other anomalies such as sacral vertebral anomalies, diastematomyelia or TCS [Figure 21].[26]

Anterior meningoceles are usually presacral in location. It has a large anterior meningocele outpouching that traverses an enlarged sacral foramen and produces a presacral cystic mass. Most ASMs are sporadic but a minority show an inherited predisposition within the Currarino triad or in syndromes that feature dural dysplasia, such as neurofibromatosis type 1 (NF1) and Marfan syndrome.

Terminal myelocystocele

Herniation of a large terminal syrinx (syringocele) into a posterior meningocele through a posterior spinal defect is referred to as a terminal myelocystocele. The terminal syrinx component communicates with the central canal, and the meningocele component communicates with the subarachnoid space. The terminal syrinx and meningocele components do not usually communicate with each other [Figure 22].

Conclusion

Spinal dysraphism includes numerous entities that vary in complexity and imaging appearance. Clinical, embryological and imaging correlation provides an organized approach in their diagnosis.

Financial support and sponsorship

Nil.

Conflicts of interest

There are no conflicts of interest.

References

1. Barkovich AJ, Millen KJ, Dobyns WB. A developmental classification of malformations of the brainstem. Ann Neurol 2007;62:625-39.
2. Parisi MA, Dobyns WB. Human malformations of the midbrain and hindbrain: Review and proposed classification scheme. Mol Genet Metab 2003;80:36-53.
3. Patel S, Barkovich AJ. Analysis and Classification of Cerebellar Malformations. Am J Neuroradiol 2002;23:1074-87.
4. Tortori-Donati P, Rossi A, Cama A. Spinal dysraphism: A review of neuroradiological features with embryological correlations and proposal for a new classification. Neuroradiology 2000;42:471-91.
5. Rufener S, Ibrahim M, Parmar HA. Imaging of Congenital Spine and Spinal Cord Malformations. Neuroimaging Clin N Am 2011;21:659-76.
6. Moore K. Congenital Abnormalities of the Spine In: Coley BD, editor. Caffey's Pediatric Diagnostic Imaging. Philadelphia, PA: Elsevier Saunders; 2013. pp 449-60.
7. Sadler TW. Embryology of neural tube development. Am J Med Genet Part C Semin Med Genet 2005;135:2-8.
8. Schoenwolf GC. Histological and ultrastructural observations of tail bud formation in the chick embryo. Anat Rec 1979;193:131-47.
9. Melvin EC, George TM, Worley G, Franklin A, Mackey J, Viles K, *et al*. Genetic studies in neural tube defects. NTD Collaborative Group. Pediatr Neurosurg 2000;32:1-9.
10. Drolet BA. Cutaneous signs of neural tube dysraphism. Pediatr Clin North Am 2000;47:813-23.
11. Rossi A, Biancheri R, Cama A, Piatelli G, Ravegnani M, Tortori-Donati P. Imaging in spine and spinal cord malformations. Eur J Radiol 2004;50:177-200.
12. Rufener SL, Ibrahim M, Raybaud CA, Parmar HA. Congenital Spine and Spinal Cord Malformations—pictorial review. Am J Roentgenol 2010;194:S26-S37.
13. Nievelstein RA, Valk J, Smit LM, Vermeij-Keers C. MR of the caudal regression syndrome: Embryologic implications. AJNR Am J Neuroradiol 1994;15:1021-9.
14. Barkovich AJ. Congenital Anomalies of the spine. In: Paediatric Neuroimaging. 3rd ed: Lippincott Williams & Wilkins; 2000. pp 650-1.

15. Tortori-Donati P, Fondelli MP, Rossi A, Raybaud CA, Cama A, Capra V. Segmental spinal dysgenesis: Neuroradiologic findings with clinical and embryologic correlation. AJNR Am J Neuroradiol 1999;20:445-56.
16. Naidich TP, Harwood-Nash DC. Diastematomyelia: Hemicord and meningeal sheaths; single and double arachnoid and dural tubes. AJNR Am J Neuroradiol 1983;4:633-6.
17. Barkovich AJ. Infections of the nervous system. In: Pediatric Neuroimaging. 4th ed ed. Philadelphia, PA: Lippincott Williams & Wilkins; 2005. pp 801-68.
18. Brown E, Matthes JC, Bazan C, 3rd, Jinkins JR. Prevalence of incidental intraspinal lipoma of the lumbosacral spine as determined by MRI. Spine (Phila Pa 1976) 1994;19:833-6.
19. Giuffre R. Intradural spinal lipomas. Review of the literature (99 cases) and report of an additional case. Acta Neurochir (Wien) 1966;14:69-95.
20. Higgins JC, Axelsen F. Simple dimple rule for sacral dimples. Am Fam Physician 2002;65:2435.
21. Kliegman RM SB, St. Geme JW, Schor NF, Behrman RE. Nelson Textbook of Pediatrics. 19th ed. Philadelphia, PA: Elsevier Saunders; 2011.
22. Castillo M. Neuroradiology Companion: Methods, Guidelines, and Imaging Fundamentals. 4th ed. Philadelphia, PA Williams and Wilkins; 2011.
23. Widjaja E, Whitby EH, Paley MN, Griffiths PD. Normal fetal lumbar spine on postmortem MR imaging. AJNR Am J Neuroradiol 2006;27:553-9.
24. Khan AN, Turnbull I, Sabih D, Al-Okaili R Imaging in Spinal Dysraphism and Myelomeningocele. Available at: http://emedicine.medscape.com/article/413899. [Last accessed on Mar 18, 2014].
25. Coleman LT, Zimmerman RA, Rorke LB. Ventriculus terminalis of the conus medullaris: MR findings in children. AJNR Am J Neuroradiol 1995;16:1421-6.
26. Lohani S, Rodriguez DP, Lidov HG, Scott RM, Proctor MR. Intrasacral meningocele in the pediatric population. J Neurosurg Pediatr 2013;11:615-22.